

# Optimal Quasi-Steady Plasma Thruster System Characteristics

DENNIS E. LUDWIG\* AND ARNOLD J. KELLY†

Princeton University, Princeton, N.J.

The over-all characteristics of a generalized Quasi-steady Plasma Thruster (QPT) system consisting of thruster head, power conditioning network, and propellant supply subsystem are studied. Energy balance equations for the system are coupled with component mass relationships in order to determine over-all system mass and performance. Power supply power levels varying from 100 to 10,000 w with thruster power levels ranging from 300 kw to 30 Mw employing argon as the propellant are considered. The manner in which over-all system mass, average thrust, and burn time vary as a function of power supply power level, quasi-steady power level, and pulse time are studied. Results indicate the existence of optimum pulse times when system mass is employed as an optimization criterion.

## Nomenclature

$e$  = one electronic charge =  $1.6 \times 10^{-19}$  coul  
 $E_{av}$  = energy available for discharge, joules  
 $E_t$  = energy dissipated in thruster, joules  
 $i$  = exponent defining matched condition for mass flow rate  
 $I_0$  = quasi-steady current level, amps  
 $I_T$  = total impulse, nt-sec  
 $K$  = constant used in determining critical  $\dot{m}_0/I_0^i$ , variable dimensions  
 $M$  = propellant molecular weight  
 $\dot{m}_0$  = quasi-steady mass flow rate, kg/sec  
 $\langle \dot{m} \rangle$  = average mass flow rate over cycle, kg/sec  
 $m$  = mass expelled per pulse, kg  
 $m_c$  = individual nonelectrolytic capacitor mass, kg  
 $m_e$  = individual electrolytic capacitor mass, kg  
 $m_i$  = total initial system mass, kg  
 $m_{in}$  = total power conditioning network mass, kg  
 $m_{mis}$  = miscellaneous lumped mass including valves, piping, insulation etc., kg  
 $m_p$  = total fuel required for mission, kg  
 $m_{ps}$  = power supply mass, kg  
 $m_{tank}$  = propellant tank mass, kg  
 $m_{th}$  = thruster head mass, kg  
 $\langle P_s \rangle$  = average power supply output power, watts  
 $P_t$  = quasi-steady power level, watts  
 $Q_{del}$  = charge delivered to thruster during  $t_p$ , coul  
 $R$  = universal gas constant = 8.314 joules/mole-°K  
 $r_a$  = anode radius, m  
 $r_c$  = cathode radius, m  
 $S_f$  = propellant tank design safety factor  
 $T$  = average propellant tank operating temperature, °K  
 $\langle T \rangle$  = average thrust over cycle, nt  
 $T_0$  = quasi-steady thrust level, nt  
 $t_b$  = burn time, months  
 $t_c$  = charge time, sec  
 $t_j$  = pulse time, sec  
 $t_p$  = total cycle time, sec  
 $V$  = quasi-steady thruster terminal voltage, volts  
 $V_a$  = anode fall voltage, volts  
 $V_b$  = electromagnetic thrust voltage, volts  
 $V_c$  = cathode voltage drop, volts  
 $V_{ch}$  = power conditioning charging voltage, volts  
 $V_f$  = residual voltage in ladder network after discharge, volts  
 $V_{rated}$  = capacitor rated voltage, volts  
 $V_{ti}$  = electrothermal thruster voltage, volts  
 $v$  = quasi-steady exhaust velocity, m/sec  
 $\langle v \rangle$  = average exhaust velocity, m/sec  
 $Z$  = quasi-steady thruster impedance, ohms

$\alpha_1$  = proportionality constant for electrolytic capacitor mass, kg/coul  
 $\alpha_2$  = proportionality constant for nonelectrolytic capacitor mass, kg/joule  
 $\beta$  = specific power supply mass, kg/w  
 $\delta$  = duty cycle  
 $\varepsilon_1$  = effective ionization energy for propellant, ev  
 $\eta_c$  = charging efficiency  
 $\eta_D$  = discharging efficiency =  $\frac{\text{thrust power out}}{\text{quasi-steady power level}}$   
 $\mu_0$  = vacuum permeability =  $1.25 \times 10^{-7}$  h/m  
 $\rho_{an}$  = thruster assembly material density, kg/m<sup>3</sup>  
 $\rho_{cat}$  = cathode assembly material density, kg/m<sup>3</sup>  
 $\rho_i$  = propellant tank material density, kg/m<sup>3</sup>  
 $\sigma_y$  = propellant tank material yield stress, nt/m<sup>2</sup>  
 $\tau_A$  = time delay between initiation of mass flow and the initiation of the discharge, sec  
 $\tau_c$  = current pulse decay time, sec  
 $\tau_E$  = mass flow decay time, sec  
 $\tau_i$  = duration of quasi-steady current level, sec  
 $\tau_m$  = duration of quasi-steady mass flow, sec  
 $\tau_Q$  = duration of steady-state thruster operation, sec  
 $\tau_r$  = current rise time, sec  
 $\tau_R$  = mass flow rise time, sec  
 $\tau_s$  = time from initiation of current pulse to reach steady-state operation, sec

## Introduction

It is well established<sup>1</sup> that magnetoplasmadynamic thrusters settle into steady-state operation after a transient phase of 0(10  $\mu$ sec) when subjected to a constant current of 0(10<sup>4</sup> amps) having a sharp onset. Such thrusters, when operated in an intermittent mode, are designated quasi-steady plasma thrusters (QPT). Because experimental evidence<sup>2</sup> indicates that the efficiency of converting input electrical energy into exhaust kinetic energy increases with operating power level, the QPT is of interest since it may be operated at high quasi-steady power levels while requiring only low average continuous power.

The QPT system consists of several subsystems (discussed in the following section) and consequently requires, as for all engineering design problems, an investigation of the compromises and tradeoffs which must be made in the subsystems' characteristics in order to attain an optimum design for a given mission or class of missions. These tradeoffs are discussed in the analysis section of this paper.

Research on the QPT has advanced sufficiently to permit formulation of an initial digital computer program using recently obtained data, and describing the general characteristics and performance of this system for use as primary propulsion.

The availability of such a model permits: 1) a determination of over-all system characteristics such as duty cycle, average thrust, average mass flow rate, and system component masses as a function of mission requirements; 2) a determination of the sensitivity of the above parameters on current and mass flow

Presented as Paper 72-456 at the AIAA 9th Electric Propulsion Conference, Bethesda, Md., April 17-19, 1972; submitted May 4, 1972; revision received September 21, 1972.

Index category: Electric and Advanced Space Propulsion.

\* Graduate Student, Department of Aerospace and Mechanical Sciences.

† Assistant Professor, Department of Aerospace and Mechanical Sciences. Member AIAA.

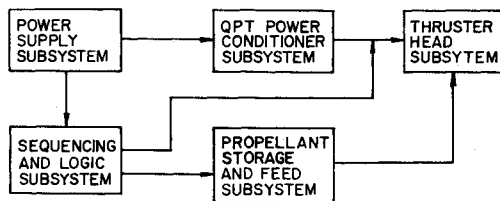


Fig. 1 QPT thruster system block diagram.

temporal behavior, power conditioning efficiencies, and quasi-steady power levels; 3) a comparison of the QPT system performance with other propulsion systems such as the ion thruster; and 4) the rational design of laboratory experiments so as to assure that the range of parameters investigated is consistent with those to be eventually encountered.

Because many of the detailed characteristics of the QPT are not documented or are currently under experimental investigation, and because the description of a pulsed system involves more parameters for a reasonable description than does a continuously operating system, a number of approximations have had to be applied to this analysis. They have been employed to reduce the number of parameters handled, to permit the identification of general trends, and to establish a base line for the development of a more comprehensive analysis.

#### General Description of the QPT Model

The model<sup>3,4</sup> presented here describes the system in terms of an energy balance and component mass relationships. The four basic subsystems of the complete QPT system which have been considered in this analysis are the following (Fig. 1): 1) power supply, 2) pulse-forming power conditioner, 3) propellant feed characteristics, and 4) coaxial plasma thruster. Variations in performance of the complete system due to such subsystems as the propellant feed power conditioner, QPT trigger unit, and QPT trigger unit power conditioner are assumed to be negligible.

The over-all system operation is indicated in Fig. 2. The power supply charges the power conditioning network at the required charging voltage for a time  $t_c$ . The energy stored in the power conditioner is then pulsed through the thruster for a time  $t_j$ . No time delays are assumed between the termination of the charging sequence and the initiation of the discharging sequence.

The relationship between the current discharge pulse and the propellant discharge pulse is assumed to follow the form indicated in Fig. 3. In order to insure that the chamber pressure is high enough so that mass starved operation (i.e., the erosion of electrodes and insulators) does not occur, the propellant flow is initiated at a time  $\tau_A$  prior to the triggering of the current pulse. Upon initiation of the current pulse, three transient phases occur: a) the time  $\tau_r$  required for the current to reach a steady value, b) the time  $\tau_c$  required for the cathode to begin emitting electrons thermionically, and c) the time  $\tau_s$  required for all electric and magnetic fields to become steady. This latter time increment is assumed to correspond to the time required for the chamber pressure to attain a constant value. Thus the

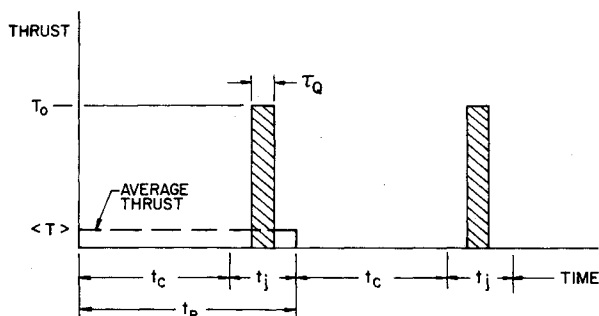


Fig. 2 Over-all QPT system operation.

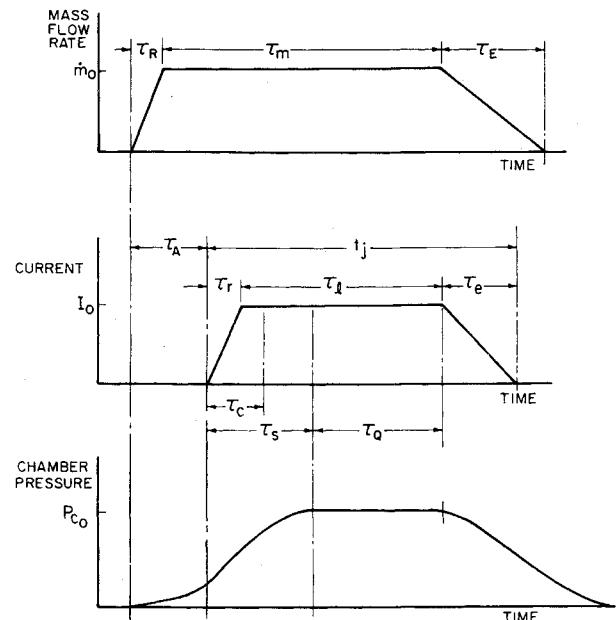


Fig. 3 Relationship between current and mass flow pulses.

thruster operates in a steady-state mode for the time increment  $\tau_Q$ . The decay of the current pulse is assumed to be initiated coincidentally with the decay of the mass flow pulse. However,  $\tau_E$  may be greater than  $\tau_e$  in order to avoid mass starved operation.

#### Power Supply Subsystem

Although in this analysis the power supply mass does not have a direct bearing on the final results, its mass is included for completeness. Typical recent power supply specific masses<sup>5</sup> are displayed in Fig. 4. The values shown are based upon the most appropriate type of power source (i.e., RTG's, turbogenerator) for a given range of values. The following relationships were developed from the data of Fig. 4:

$$\beta(\text{kg/w}) = 0.236, \quad \text{when } \langle P_s \rangle \leq 250 \text{ W} \quad (1a)$$

$$\beta(\text{kg/w}) = 1.406(\langle P_s \rangle)^{-0.323}, \quad \text{when } 250 < \langle P_s \rangle \leq 3000 \text{ W} \quad (1b)$$

$$\beta(\text{kg/w}) = 24.1(\langle P_s \rangle)^{-0.675}, \quad \text{when } \langle P_s \rangle > 3000 \text{ W} \quad (1c)$$

#### Propellant Storage and Feed Subsystem

Efficient operation of the QPT occurs when the propellant mass flow rate is "matched" with the current level. This condition generally occurs when the voltage across the thruster head is well defined and free from high-frequency noise during the discharge pulse. This matched condition also results in very low levels of ablation of the anode, cathode, and insulators. For a given current level, unmatched operation occurs for a

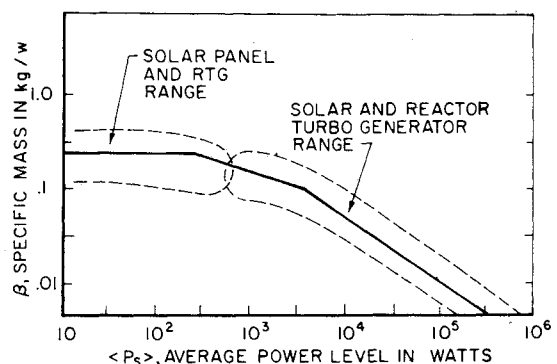


Fig. 4 Capability of space power systems under development.

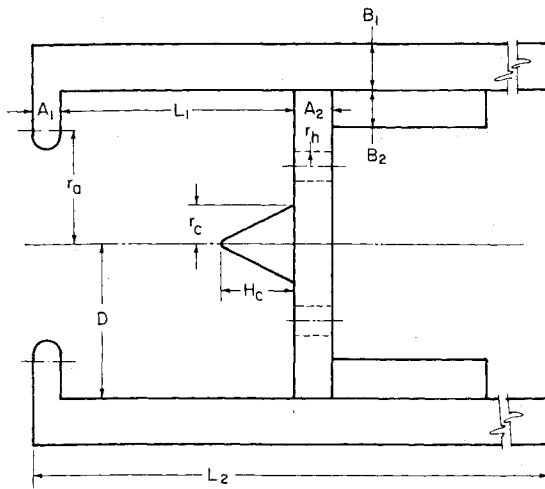


Fig. 5 Simplified thruster head geometry.

slightly lower mass flow rate, and it is typified by significant ablation and an erratic voltage response. Certain theoretical arguments<sup>6</sup> suggest that this matched mass flow rate is proportional to the square of the quasi-steady current, although at present the experimental evidence seems to follow this relationship only approximately.

For the present study, however, it is assumed that the matched flow rate is proportional to the square of the current, and that ablation of the anode, cathode, and insulators is negligible. The rise, decay, and steady flow times of the mass pulse are assumed to be known functions or are functions of the current profile.

In keeping with the level of accuracy of the other subsystem descriptions in the model, a simple spherical propellant pressure vessel in which the wall thickness is much less than the vessel diameter has been assumed. The vessel and propellant are assumed to be kept at an average known operating temperature and the initial pressure is  $\frac{2}{3}$  the yield stress of the vessel material.

Since the actual design of the system is variable and has yet to be determined, all equipment such as valves, piping, etc., are lumped into one constant given mass ( $M_{mis}$ ).

The propellant feed properties are represented by the following relationships:

$$\dot{m}_0 = KI_0^i \quad (2)$$

$$m = \dot{m}_0[\tau_m + (\tau_E + \tau_R)/2] \quad (3)$$

$$\langle \dot{m} \rangle = m/t_p \quad (4)$$

$$m_p = t_b \langle \dot{m} \rangle \quad (5)$$

$$m_{\text{tank}} = m_p(1.5\rho_t(R)(T)(S_f)/(\sigma_y M) \quad (6)$$

It should be pointed out that the parameter  $i$  in Eq. (2) has been introduced to permit the influence of various matching conditions to be investigated. As was pointed out earlier, the most accurate and commonly applied criterion to date corresponds to  $i = 2$  (i.e.,  $\dot{m}_0 \propto I_0^2$ ).

### Thruster Head Subsystem

Thrust is considered to be produced only for the time increment  $\tau_0$  during which the electric and magnetic fields are steady in the thruster head, and during which the cathode is emitting electrons thermionically. Also, this model considers only the electromagnetic component of the thrust [Eq. (13)] and does not include the gasdynamic and electrothermal components. These assumptions then give a conservative estimate of both the quasi-steady and the average thrust.

In this analysis, the thruster head geometry (see Fig. 5) is assumed to remain constant. The following equations are used to describe the thruster head operation during discharge:

$$V_a = 15 \quad (7)$$

$$V_c = 5 \quad (8)$$

$$V_b = T_0^2/(2\dot{m}_0 I_0) \quad (9)$$

$$V_i = \dot{m}_0 e \epsilon_1 / [M(1.66 \times 10^{-27}) I_0] \quad (10)$$

$$V = V_0 + V_c + V_b + V_i \\ = V_0 + V_c + AI_0^{3-i} + BI_0^{i-1} \quad (11)$$

$$P_t = (V_a + V_c)I_0 + AI_0^{4-i} + BI_0^i \quad (12)$$

$$T_0 = \mu_0 I_0^2 [\ln(r_a/r_c) + 0.75]/(4\pi) \quad (13)$$

$$Z = V/I_0 \quad (14)$$

$$m_{\text{th}} = \pi[\rho_{an}(2DB_1 + B_1^2)L_2 + (2DB_2 - B_2^2) \cdot \\ (L_2 - L_1 - A_2) + (D^2 - 6r_h^2)A_2 + \\ (D^2 - r_a^2)A_1] + \rho_{cat}(r_c^2 H_c \pi/3) \quad (15)$$

where for convenience we have let

$$A = [\mu_0^2/32\pi^2 K][\ln(r_a/r_c) + 0.75]^2 \quad (16)$$

$$B = K e \epsilon_1 / [M(1.66 \times 10^{-27})] \quad (17)$$

The power consumed by the thruster [cf. Eq. (12)] can be broken down into four components: 1) the power dissipated at the anode,  $V_a I_0$ , 2) the power dissipated at the cathode,  $V_c I_0$ , 3) the electrothermal power,  $V_i I_0$ , consumed during ionization and heating of the gas, and 4) the electromagnetic thrust power,  $V_b I_0$ , consumed during electromagnetic acceleration of the ionized gas. The anode and cathode voltage drops have been experimentally determined to be approximately constant, and are assumed constant in this analysis.

The value of  $\epsilon_1$  (the average energy expended in producing one ion) is not fully understood. Strong experimental evidence suggests that its value may be an order of magnitude higher than the propellant's first ionization energy. However, for the purposes of this initial baseline study, the use of the first ionization energy for  $\epsilon_1$  is adequate.

### Power Conditioning Subsystem

The power conditioning equipment is essentially a pulse-forming network. Typically, it is a lumped parameter transmission line or ladder network. The performance characteristics (namely the rise, steady state, and decay times, quasi-steady power levels, charging and discharging efficiencies, charging and final network voltages) of lossless or only slightly lossy networks (i.e., networks using nonelectrolytic capacitors) is well defined. However, the performance of networks using electrolytic capacitors is neither well defined nor amenable to analytic analysis. Consequently, it is assumed that these characteristics are determined separately either experimentally or numerically and are specified as input data.

Indeed, it would be inappropriate to include in the model an analysis of ladder networks, since this would represent a degree of sophistication inconsistent with the purposes of this preliminary work. Ducati<sup>7</sup> has found that the networks whose schematics are shown in Fig. 6 are promising contenders for the

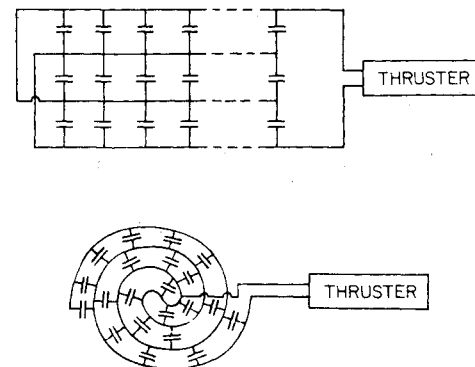


Fig. 6 Experimental power conditioners.

role of power conditioner. These circuits take advantage of mutual inductance effects which would lead to obvious complexity in any modeling attempt.

The energy delivered to the thruster during discharge [Eq. (20) in this section] is calculated by analytical integration of the power equation [Eq. (12)], which has been assumed valid over the entire pulse period. The mass relationships for capacitors as presented by Wilbur<sup>8</sup> are assumed valid in the present analysis. The inductor masses are not considered negligible, but because nothing is known at present about the type of power conditioner which will be used, inductor masses are assumed to be included with the capacitor mass relationships by means of proportionality constants ( $\alpha_1, \alpha_2$ ).

The following equations are associated with the power conditioner:

$$Q_{del} = I_0[\tau_i + (\tau_r + \tau_e)/2] \quad (18)$$

$$\eta_D = E_i/E_{av} \quad (19)$$

$$E_{av} = \{(V_a + V_c)[\tau_i + (\tau_r + \tau_e)/2]I_0 + A[\tau_i + (\tau_r + \tau_e)/(5-i)]I_0^{(4-i)} + B[\tau_i + (\tau_r + \tau_e)/(i+1)]I_0^i\}/\eta_D \quad (20)$$

$$m_e = \alpha_1 Q_{del}[V_{rated}/(V_{ch} - V_f)] \quad (21)$$

$$m_c = \alpha_2 (Q_{del}/2)[V_{rated}^2/(V_{ch} - V_f)] \quad (22)$$

$$\eta_e = E_{av}/(\langle P_s \rangle t_c) \quad (23)$$

#### Over-All QPT System Characteristics

With the preceding equations and assumptions in mind, the over-all system performance characteristics can now be written (cf. Fig. 3):

$$t_j = \tau_i + \tau_r + \tau_e \quad (24)$$

$$\delta = t_j/(t_c + t_j) \quad (25)$$

$$\tau_Q = \tau_r + \tau_i - \tau_s \quad (26)$$

$$\tau_s = a/I_0 + \tau_r \text{ (an empirical result)} \quad (27)$$

$$t_p = t_j + t_c \quad (28)$$

$$\langle T \rangle = T_0 \tau_Q/t_p \quad (29)$$

$$\langle \dot{m} \rangle = m/t_p \quad (30)$$

$$\langle V \rangle = \langle T \rangle / \langle \dot{m} \rangle \text{ (effective)} \quad (31)$$

$$\eta_T = V_b/V \quad (32)$$

$$m_i = m_{in} + m_{th} + m_p + m_{tank} + m_{ps} + m_{mis} \quad (33)$$

#### Assumptions for the Present Study

The purpose of this paper is to present the results of an analysis of an "ideal" system using lossless electrolytic capacitors. That is, the pulse shapes are assumed rectangular, and the efficiencies are assumed to be unity. This analysis can thus be viewed as presenting reference or base-line performance trends. However, it is anticipated that despite the simplifying assumptions employed, actual thruster systems will reflect the trends and fundamental results of this analysis.

The following assumptions have been employed in analyzing the ideal QPT system using argon as the propellant:

$$i = 2$$

$$\epsilon_1 = 15.75 \text{ eV}$$

$$K = 2.7 \times 10^{-11} \text{ kg/(amp}^2\text{-sec)}$$

$$\tau_r = \tau_R = 0$$

$$\tau_e = \tau_E = 0$$

$$\tau_A = 0$$

$$\tau_s = a/I_0, a = 0.5 \text{ coul}$$

$$\tau_Q = t_j - a/I_0$$

$$\eta_D = \eta_c = 1$$

$$V_{rate} = 520 \text{ volts}$$

$$V_{ch} = 2V \text{ volts}$$

$$V_f = V \text{ volts}$$

The last two conditions result from the case of a lossless ladder network matched with the load. The final voltage is assumed to be the thruster terminal voltage since the current is abruptly terminated at this value.

This analysis has assumed a typical stainless steel propellant tank maintained at a temperature of 293°K. The thruster head assembly is aluminum, and the cathode is tungsten. The anode to cathode radius ( $r_a/r_c$ ) is 5. The lumped mass ( $m_{mis}$ ) is arbitrarily taken as 20 kg, and the safety factor  $s_f$  is 1.5.

#### Analysis

Several important features of the ideal system performance should be noted:

1) For a given total impulse and a given instantaneous thruster power level, a minimum in total system mass does occur (Figs. 7a, b, c). This results from a tradeoff in fuel mass and power conditioning mass. For pulse times to the left of the minimum, the fuel mass dominates the system, and for pulse times to the right of the minimum, the power conditioning mass dominates. This is a direct consequence of the behavior of Eqs. (26) and (27), which indicate that as the pulse length approaches  $\tau_s$ , the average thrust approaches zero, implying infinite burn time and thus infinite propellant (since the pulse length is not zero).

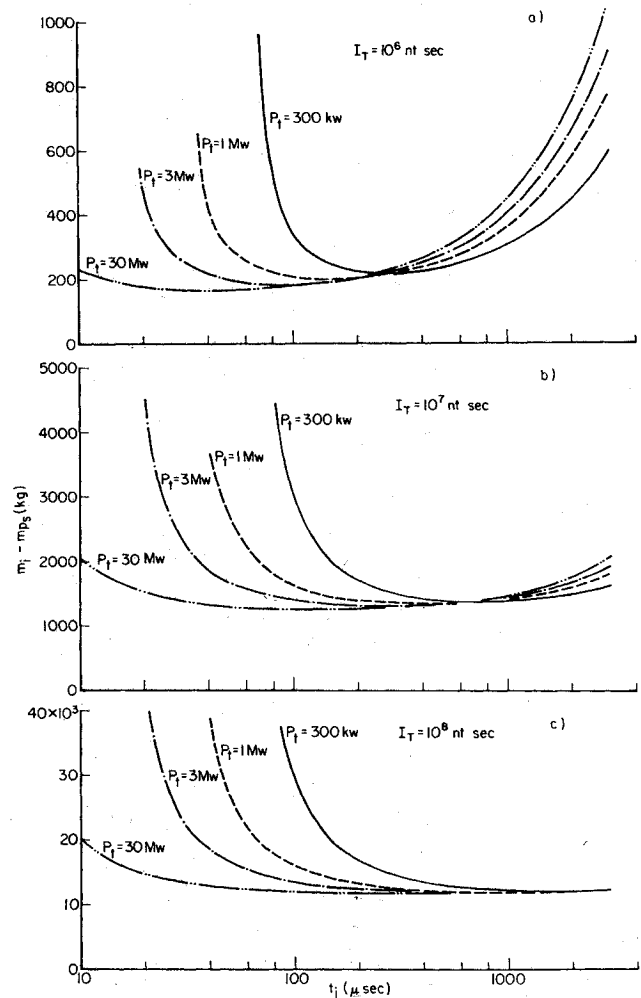


Fig. 7 System mass minus power supply mass vs pulse length.

2) For a given total impulse, the pulse time at which minimum system mass occurs shifts to lower values as the instantaneous thruster power level increases. As  $P_t$  goes up,  $\tau_s$  decreases and  $\tau_0$  increases, implying that more efficient use is made of a given pulse. That is, the average thrust goes up, the burn time goes down, and thus less propellant is required (cf. Fig. 3).

3) It is also apparent that for a fixed total impulse, the minimum system mass is reduced slightly as  $P_t$  increases. This is a result of the decrease in required power conditioning mass. As  $P_t$  increases, the thruster operating voltage increases. For this ideal case, the initial power conditioning charging voltage is twice the thruster operating voltage. Equation (21) indicates that for a fixed rated voltage, and a fixed charge delivered, the capacitor mass will go down as the charging voltage approaches the rated voltage.

4) The minimum system mass point does not remain stationary as total impulse increases. For a fixed  $P_t$ , this point shifts to longer pulse lengths. This is a consequence of the fact that the propellant becomes a larger fraction of the total mass as specific impulse increases.

5) Since the propellant and power conditioning masses are not functions of power supply power, the power supply mass is simply an additive constant to each constant  $P_t$  curve. Figure 4 may be used to determine the required power supply mass.

Further characteristics may be determined from Fig. 8 and Fig. 9: 6) The curves are altered only when the power supply output is not negligible compared to the quasi-steady power level. 7) For a fixed  $\langle P_s \rangle$  and  $P_t$ , an increase in total impulse means an increase in burn time, since the average thrust is constant for a fixed cycle time. 8) For a fixed total impulse and  $P_t$ , an increase in  $\langle P_s \rangle$  means a decrease in burn time since, for a given pulse time, the average thrust increases with increasing  $\langle P_s \rangle$ . 9) An increase in quasi-steady thruster power means an increase in average thrust implying a decrease in burn time, for all other parameters held constant. 10) For a given  $P_t$ , an increase in pulse length means an increase in average thrust implying a decrease in burn time, for all other parameters held constant.

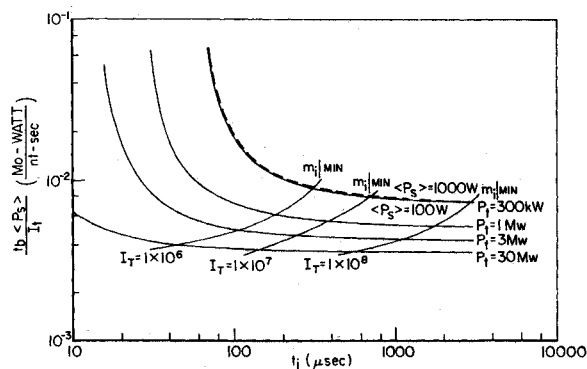


Fig. 8 Universal burn time parameter vs pulse length.

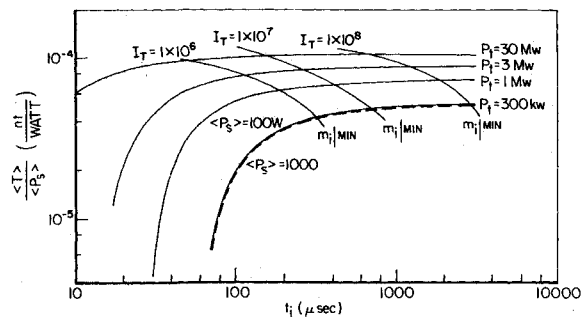


Fig. 9 Thrust parameter vs pulse length.

## Conclusions

Within the context of this idealized analysis, the following conclusions regarding the overall operation of the QPT system can be drawn: 1) For all cases considered, operation of the system between the pulse time ranges of 200  $\mu\text{sec}$  and 600  $\mu\text{sec}$  means that the system is near its point of minimum mass. 2) Under the same operating conditions as above, the average thrust is near its asymptotic maximum, and the burn time is near its asymptotic minimum. 3) Increasing the quasi-steady power level moves the position of minimum system mass to shorter pulse times. 4) An order-of-magnitude increase in quasi-steady power level implies neither an order-of-magnitude increase in thrust, nor an order-of-magnitude decrease in burn time.

## References

- Clark, K. E. and Jahn, R. G., "Quasi-Steady Plasma Acceleration," *AIAA Journal*, Vol. 8, No. 2, Feb. 1970, pp. 216-220.
- Hoell, J. M., Burlock, J., and Jarrett, O., "Velocity and Thrusts Measurements in a Quasi-Steady Magnetoplasmadynamic Thruster," *AIAA Journal*, Vol. 9, No. 10, Oct. 1971, pp. 1969-1974.
- Kelly, A. J., "Preliminary Description of the Quasi-Steady Plasma Thruster as a Primary Propulsion System," ASAR Memo 38, Oct. 1970, Dept. of Aerospace and Mechanical Sciences, Princeton University, Princeton, N. J.
- Clark, K. E., "Quasi-Steady Plasma Acceleration," Rept. 859, May 1969, Aerospace and Mechanical Sciences, Princeton University, Princeton, N. J.
- Szego, G. C., "Space Power Systems," Part 1, AGARDograph 123, Nov. 1969, Advisory Group for Aerospace Research and Development, NATO, p. 84.
- Malliaris, A. C., John, R. R., Garrison, R. L., and Libby, D. R., "Quasi-Steady MPD Propulsion at High Power," CR-111872, Feb. 1971, NASA.
- Ducati, A. C. and Jahn, R. G., "Investigation of Pulsed Quasi-Steady MPD Arc Jets," CR-111970, June 1971, NASA.
- Wilbur, P. J., "Electrolytic Capacitor Current Pulse Networks for Quasi-Steady MPD Arcs," *AIAA Journal*, Vol. 9, No. 8, Aug. 1971, pp. 1447-1451.